Contrib Mineral Petrol (2004) 146: 762–778
DOI 10.1007/s00410-003-0533-3

ORIGINAL PAPER

David Dolejš · Don R. Baker

Thermodynamic analysis of the system Na_2O-K_2O-CaO-Al_2O_3-SiO_2-H_2O-F_2O_{-1}: Stability of fluorine-bearing minerals in felsic igneous suites

Received: 18 December 2002 / Accepted: 24 October 2003 / Published online: 6 December 2003
© Springer-Verlag 2003

Abstract Thermodynamic analysis of the system Na_2O-K_2O-CaO-Al_2O_3-SiO_2-H_2O-F_2O_{-1} provides phase equilibria and solidus compatibilities of rock-forming silicates and fluorides in evolved granitic systems and associated hydrothermal processes. The interaction of fluorine with aluminosilicate melts and solids corresponds to progressive fluorination of their constituent oxides by the thermodynamic component F_2O_{-1}. The chemical potential $\mu(F_2O_{-1})$ buffered by reaction of the type: $MO_{n/2}$ (s) + n/2 $[F_2O_{-1}] = MF_n$ (s, g) where M = K, Na, Ca, Al, Si, explains the sequential formation of fluorides: carobbiite, villiaumite, fluorite, AlF_3, SiF_4 as well as the common coexistence of alkali- and alkali-earth fluorides with rock-forming aluminosilicates. Formation of fluorine-bearing minerals first starts in peralkaline silica-undersaturated, proceeds in peraluminous silica-oversaturated compositions and causes progressive destabilization of nepheline, albite and quartz, in favour of villiaumite, cryolite, topaz, chiolite. Additionally, it implies the increase of buffered fluorine solubilities in silicate melts or aqueous fluids from peralkaline silica-undersaturated to peraluminous silica-oversaturated environments. Subsolidus equilibria reveal several incompatibilities: (i) topaz is unstable with nepheline or villiaumite; (ii) chiolite is not compatible with albite because it only occurs only at very high F_2O_{-1} levels. The stability of topaz, fluorite, cryolite and villiaumite in natural felsic systems is related to their peralkalinity (peraluminosity), calcia and silica activity, and linked by corresponding chemical potentials to rock-forming mineral buffers. Villiaumite is stable in strongly peralkaline and Ca-poor compositions ($An_{<0.001}$). Similarly, cryolite stability requires coexistence with nearly-pure albite ($An_{<2}$). Granitic rocks with Ca-bearing plagioclase ($An_{>5}$) saturate with topaz or fluorite. Crystallization of topaz is restricted to peraluminous conditions, consistent with the presence of Li-micas or anhydrous aluminosilicates (cordierite, garnet, andalusite). Fluorite is predicted to be stable in peraluminous biotite granites, amphibole-, clinopyroxene- or titanite-bearing calc-alkaline suites as well as in peralkaline granitic and syenitic rocks. Fluorine concentrations in felsic melts buffered by the coexistence of F-bearing minerals and feldspars increase from peralkaline through metaluminous to mildly peraluminous compositions. At low-temperature conditions, the hydrothermal evolution of peraluminous granitic and greisen systems is controlled by white mica-feldspar-fluoride equilibria. With decreasing temperature, topaz gradually breaks down via: (i) $(OH)F_{-1}$ substitution and fluorine transfer to fluorite by decalcification of plagioclase below 600 °C, (ii) formation of muscovite and additional fluorite at 475–315 °C, and (iii) formation of paragonite and cryolite, consuming F-rich topaz and albite below 315 °C. These equilibria explain the absence of magmatic fluorite in Ca-bearing topaz granitic rocks; its abundance in hydrothermal rocks is due to: (i) closed-system defluorination of topaz, (ii) open-system decalcification of plagioclase or (iii) hydrolytic alteration. These results provide a complete framework for the investigation of fluorine-bearing mineral stabilities in felsic igneous suites.

Editorial responsibility: T.L. Grove

Electronic Supplementary Material Supplementary material is available in the online version of this article at http://dx.doi.org/10.1007/s00410-003-0533-3. A link in the frame on the left on that page takes you directly to the supplementary material.

D. Dolejš (✉) · D. R. Baker
Earth and Planetary Sciences,
McGill University, 3450 rue University,
Montréal, H3A 2A7, Canada
E-mail: dolejs@eps.mcgill.ca
Fax: +1-514-3984680

Introduction

Highly differentiated granitic systems often exhibit elevated fluorine concentrations (Bailey 1977; London 1997), which have profound effects on the chemical and physical properties of these evolved melts. Levels of

fluorine enrichment increase in prolonged fractionation sequences (Fig. 1) from biotite granites (average: 0.11 ± 0.07 wt% F), through topaz rhyolites and granites (0.89 ± 0.57 and 1.09 ± 0.69 wt% F, respectively) to quartz topazites (3.85 ± 2.12 wt% F). Individual fluorine concentrations in melt inclusions (e.g. Webster and Duffield 1994; Webster et al. 1997; Thomas and Klemm 1997; Thomas et al. 2000) vary from 0.2 to ~5 wt% (~40 mol%) F. Furthermore, distinctly different concentrations of fluorine in solidified granites and rhyolites (0.99 ± 0.89 wt% F) and their melt inclusions (3.10 ± 1.12 wt% F) attest to significant partitioning of fluorine into hydrothermal fluids and its incorporation into greisens (2.58 ± 1.79 wt% F).

Fluorine is incorporated in a variety of minerals: fluorite, topaz, cryolite, villiaumite, chiolite, malladrite, carobbiite etc. (Bailey 1980). These occurrences span peraluminous and peralkaline igneous suites (Horbe et al. 1991; Marshall et al. 1998; Pauly and Bailey 1999), pegmatites (London 1987), greisen or skarn aureoles (Pollard et al. 1987; Štemprok 1987; Burt 1972) and orthometamorphics (Bohlen and Essene 1978).

Despite the widespread natural occurrence and the vast body of physical-chemical studies on F-bearing systems, the fundamental controls of crystallization of F-bearing minerals in magmatic environments remain unknown. In previous studies (Bohlen and Essene 1978; Burt 1981; Burt and London 1982), the availability of thermodynamic data was very limited and often restricted to one-atmosphere pressure (Stormer and Carmichael 1970). More recent thermodynamic assessments (Barton 1982; Anovitz et al. 1987; Zhu and Sverjensky 1991), combined with recent optimizations of alkali aluminosilicate systems (Eriksson et al. 1993; Wu et al. 1993) require critical evaluation for internal consistency, but provide the starting point for assessing stabilities and crystallization conditions of F-bearing phases in diverse natural multicomponent systems.

In this paper, we critically evaluate and present a complete thermodynamic dataset for solid and gaseous species in the system Na_2O-K_2O-CaO-Al_2O_3-SiO_2-H_2O-F_2O_{-1} at elevated temperatures and pressures and calculate compatibilities between major rock-forming minerals and common F-bearing phases. The effect of fluorine on silicate equilibria is developed in the simple quaternary systems Na_2O-Al_2O_3-SiO_2-F_2O_{-1}, K_2O-Al_2O_3-SiO_2-F_2O_{-1} and CaO-Al_2O_3-SiO_2-F_2O_{-1}. Rock-forming mineral buffers provide chemical potentials of system components (e.g. Na_2O, CaO, Al_2O_3) which dictate the stabilites of topaz, cryolite, fluorite and villiaumite in natural multicomponent systems (see eText 1). These results provide a comprehensive treatment of the stabilities of F-bearing phases in felsic magmas, as well as their transformations during subsolidus conditions.

The application of equilibrium thermodynamics provides a starting point for evaluating the origin of natural F-bearing assemblages as well as for recognizing

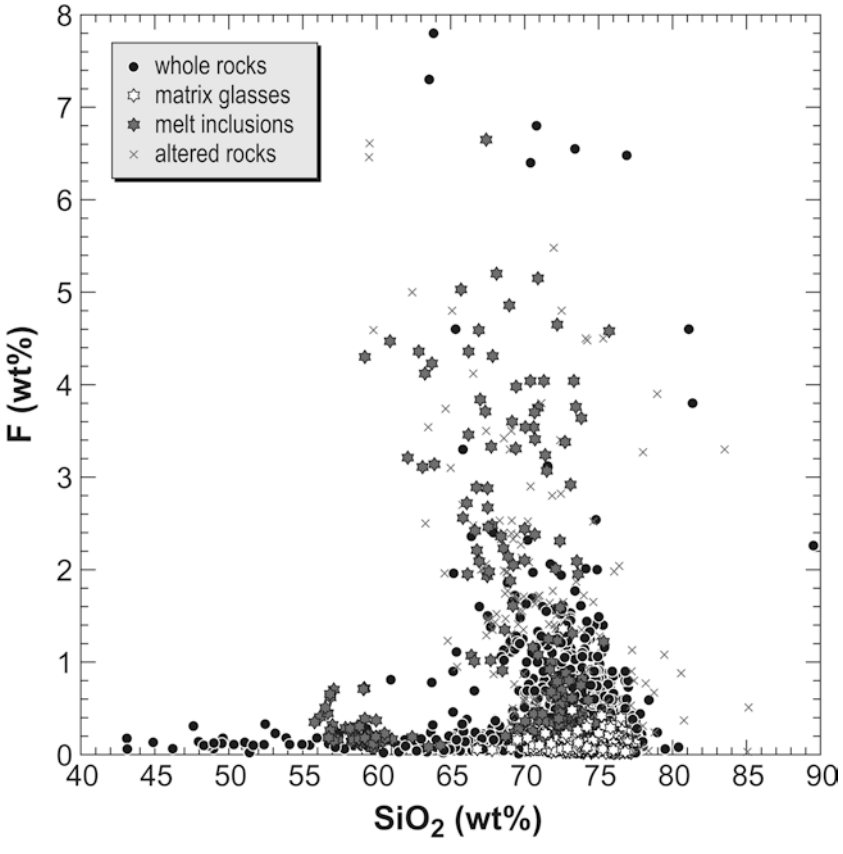

Fig. 1 Fluorine concentrations in igneous rocks, matrix glasses, melt inclusions and hydrothermally altered rocks (for data sources, see eAppendix 1)

potential disequilibrium relationships. Previous utilization of phase-equilibria involving F-bearing phases (e.g. Aksyuk 1995; Halter and Williams-Jones 1999; Sallet 2000) yielded consistent results with pressure-temperature estimates based on rock-forming phases (e.g. Sallet 2000; Anderson 1996) and provides further promise for the applicability of the equilibrium concept to volatile-bearing igneous systems.

Thermodynamic dataset

Thermodynamic properties of solid and gaseous species in the system Na_2O-K_2O-CaO-Al_2O_3-SiO_2-H_2O-F_2O_{-1} were compiled from the following sources—Holland and Powell (1998): rock-forming minerals, H_2O; FACT thermodynamic database (Bale et al. 2002): alkali silicates (Wu et al. 1993), alkali aluminates (Eriksson et al. 1993), Na-Ca-K fluorides (Chartrand and Pelton 2001); Chase (1998): aluminofluorides, and Barton et al. (1982): topaz. The volumetric data were retrieved from crystal-structure refinements (eTable 1).

The FACT database is based on thermochemical compilations by Barin (1993) and Chase (1998) and is optimized by evaluating experimental phase equilibria for internal consistency. The corresponding mineral dataset has been selected according to consistency with calorimetric studies. Previous datasets by Helgeson et al. (1978) and Berman (1988) require enthalpic adjustments by −1,000 J/mol and −6,700 to −6,800 J/mol, respectively, to fit experimental solubility equilibria and precisely known properties of aqueous ions (Sverjensky et al. 1991). These adjustments, coincidentally, bring the above datasets to a much closer agreement with recent data of Holland and Powell (1998). The thermodynamic data by Holland and Powell (1998) are preferred for additional reasons: (i) consistency with feldspar calorimetric data (Navrotsky et al. 1980; Kiseleva et al. 1990; Robie and Hemingway 1995), and (ii) consistency with aqueous and dissociation equilibria (Anderson et al. 1991; Sverjensky et al. 1991).

The thermodynamic data for topaz (Barton et al. 1982) have been adjusted ($\Delta_f G$ and $\Delta_f H$ increased by 6,400 J/mol) to provide internal consistency with hydroxytopaz (Holland and Powell 1998). Thermodynamic data for fluoromuscovite (Zhu and Sverjensky 1991) appear to significantly overestimate the stability of muscovite solid solution and were not included in the calculation. Cryolite was considered as a stoichiometric Na_3AlF_6 phase, however it exhibits a minor solid solution towards AlF_3 above 600 °C (Dewing 1997). Behavior of H_2O was described by the compensated Redlich-Kwong equation (Holland and Powell 1991, 1998) and fluoride gaseous species (SiF_4, $NaAlF_4$) were treated as ideal gases (fugacity = total pressure). The thermodynamic properties of all species in the system Na_2O-K_2O-CaO-Al_2O_3-SiO_2-H_2O-F_2O_{-1}, supplementing the internally consistent database of Holland and Powell (1998), are presented in eTables 1 and 2.

Several mineral phases form solid solutions and were described by the following solution models: feldspars—ternary asymmetric model (Fuhrman and Lindsley 1988; as corrected in Wen and Nekvasil 1994), white mica—non-ideal asymmetric model (Chatterjee and Froese 1975), topaz—ideal proton-avoidance model (Barton 1982), and Ca-Mg-amphibole—symmetric binary solution (Dale et al. 2000).

Total errors involved in present thermodynamic analysis reflect the quality of end-member data, inter-database consistency and error propagation in reaction calculations. Standard-state thermodynamic properties of rock-forming silicates are accurate to ±3 kJ/mol (Holland and Powell 1998), data of fluortopaz are known to ±4.4 kJ/mol (Barton 1982), and properties of silicate, aluminate and fluoride species are accurate to ±6 kJ/mol (Chase 1998). The Gibbs free energies calculated from the FACT database (Bale et al. 2002) and the JANAF thermochemical tables (Chase 1998) are consistent to ±3 kJ, i.e. within error brackets. Error propagation in reaction equilibria leads to uncertainties of 7 kJ/mol in estimates of $\Delta_r G$ and $\mu(F_2O_{-1})$.

Throughout the presentation, we use chemical potentials rather than activities of mobile components. The advantages are twofold: (i) the calculation of activities requires the choice of appropriate standard state, commonly a pure liquid or solid phase at P and T of interest. For several species, such a standard state is either hypothetical (e.g. F_2O_{-1}) or has no obvious relation to the presence or activities of major rock-forming minerals (e.g. Na_2O, CaO). The use of chemical potentials, which are defined by the system itself, rather than activities, avoids unnecessary standard-state conventions. (ii) if $\Delta_r G_{solids}$ changes negligibly over an arbitrary temperature range (e.g. quartz-plagioclase equilibria), the chemical potential of mobile component remains approximately constant. On the contrary, the activity of mobile species will change appreciably, since it assimilates the inverse correlation with temperature: $\ln a \sim -\Delta_r G_{solids}/RT$. The utilization of chemical potentials prevents artificial shifts of phase-diagram topology related to the change of temperature.

Thermodynamic component F_2O_{-1}

The thermodynamic component F_2O_{-1} represents replacement of one oxygen anion by two fluorine anions while maintaining charge balance and redox state (Burt 1972). This "anion exchange operator" (Burt 1974) describes progressive fluorination of oxides or silicates into fluorides and topaz, e.g. andalusite-topaz equilibrium is represented as $Al_2SiO_5 + [F_2O_{-1}] = Al_2SiO_4F_2$, whereas the use of elemental components (i.e. F_2) requires an unnecessary consideration of redox reactions (Burt and London 1982; cf. Anovitz et al. 1987). Due to its hypothetical nature, F_2O_{-1} does not have a standard state and hence its activity (if necessary) must be related to some reference equilibrium at arbitrary P and T, e.g.

$Al_2O_3 + 3\ [F_2O_{-1}] = 2\ AlF_3$ (Anovitz et al. 1987) or $SiO_2 + 2\ [F_2O_{-1}] = SiF_4$ (this study).

Simple equilibria allow F_2O_{-1} to be converted to monitors of fluorine concentrations or activity. The component F_2O_{-1} is the hydrofluoric acid anhydride (cf. Burt 1976a) and is related to HF through the equilibrium:

$$H_2O + [F_2O_{-1}] = HF^0\ (aq)$$

HF^0 is an important fluoride species in high-temperature hydrothermal fluids associated with peraluminous systems (Halter et al. 1998). The quasichemical approach incorporates a model for fluorine solubility in silicate melts (Pelton 1999). Using the Na_2O-CaO-SiO_2 system as an example:

$$Na_2O\ (l) + [F_2O_{-1}] = 2\ NaF\ (l)$$

$$CaO\ (l) + [F_2O_{-1}] = CaF_2\ (l)$$

The thermodynamic properties of oxide, silicate (Ghiorso and Sack 1995; Pelton 1997; Holland and Powell 2001) and fluoride species (Chartrand and Pelton 2001) combined with the assumption of ideal-mixing of O^{2-}, O^- and F^- on the anion sublattice of the silicate melt structure (Pelton 1999) provide a satisfactory estimate of proportions of liquid fluoride species and therefore the total fluorine concentration in the silicate melt.

For solid-solid equilibria the chemical potential of F_2O_{-1} provides consistency between independent estimates of "fluorine concentration" from silicate-fluoride buffers and OH-F solid solutions, for example (cf. Burt 1972, 1981):

$$[F_2O_{-1}] + CaSiO_3\ (wollastonite) = CaF_2\ (fluorite) + SiO_2\ (quartz)$$

$$[F_2O_{-1}] + CaMgSi_2O_6\ (clinopyroxene) = CaF_2\ (fluorite) + MgSiO_3\ (orthopyroxene) + SiO_2\ (quartz)$$

$$[F_2O_{-1}] + Al_2SiO_4(OH)_2\ (topaz, ss) = Al_2SiO_4F_2\ (topaz, ss) + H_2O$$

$$[F_2O_{-1}] + KMg_3AlSi_3O_{10}(OH)_2\ (biotite, ss) = KMg_3AlSi_3O_{10}F_2\ (biotite, ss) + H_2O$$

This extensive set of equilibria provides essential relationships for both (i) evaluating stabilities of F-bearing minerals in multicomponent silicate systems, and (ii) extracting information on system variables from natural assemblages.

Fluorination of oxides and silicates

Inorganic fluorides display a wide range of physical and chemical properties, which affect their occurrence and stability in natural environments. A pronounced increase in volatility towards AlF_3 and SiF_4 associated with small heats of fusion or vaporization is related to change in their structural properties; the cation coordination changes from tetrahedral (Si) to octahedral (Al, Na, K) or cubic (Ca). Similarly, the bond character varies from normal covalent M-F (e.g. SiF_4) to extremely ionic M^+F^- (e.g. NaF, KF) and increases the stability of ionic alkali fluorides. The structure of solid SiF_4 corresponds to tetrahedral molecules (bond strength = 1) attracted by van der Waals interactions (Pauling 1970), causing high volatility, whereas solid fluorides: AlF_3, villiaumite, carobbiite and fluorite form a framework of edge-sharing octahedra (bond strength = 0.17) and cubes (bond strength = 0.25), respectively (Strunz and Nickel 2001). These properties suggest the widespread stability of alkali and alkali-aluminum fluorides, the rarity of fluoroaluminosilicates and the volatility of silicon (oxy-)fluorides, and are reflected in thermochemistry of fluorides. Chemical potentials of F_2O_{-1} buffered by oxide-fluoride pairs according to $MO_{n/2} + n/2\ [F_2O_{-1}] = MF_n$ (M = K, Na, Ca, Al, Si) systematically increase with the ionic potential (Z/r) of cation M (eFig. 1) and lead to sequential formation of fluorides. At low $\mu(F_2O_{-1})$, from −779 to −731 kJ, carobbiite will coexist with solid Na_2O or Na-silicates (see below). At moderate $\mu(F_2O_{-1})$, from −730 to−594 kJ, alkali fluorides—villiaumite and carobbiite will coexist with Ca-aluminosilicate assemblages. At high $\mu(F_2O_{-1})$, from −593 to −451 kJ, fluorite and alkali fluorides become fluorine-saturating phases for aluminosilicate assemblages. In an internally buffered system at constant $\mu(F_2O_{-1})$, the activities of fluoride species will decrease in the following order: KF > NaF > CaF_2 > AlF_3 > SiF_4.

The differences in $\mu(F_2O_{-1})$ of alkali-oxide, Al_2O_3 and SiO_2 fluorination reactions (eFig. 1) also imply compatibilities of alkali, subaluminous and aluminum silicates with fluorides and topaz (eFig. 2). Na-silicates undergo fluorination into villiaumite at lowest levels of $\mu(F_2O_{-1})$, whereas Al-silicates are converted into topaz at high $\mu(F_2O_{-1})$. Consequently, villiaumite will coexist with subaluminous or peraluminous silicate assemblages over a wide range of $a(F_2O_{-1})$, i.e. fluorine concentrations. On the contrary, AlF_3 and SiF_4 are unstable with feldspars or feldspathoids (eFig. 2). The vaporization of SiO_2 in the form of SiF_4 represents the maximum limit of $\mu(F_2O_{-1})$.

Phase equilibria in the system Na_2O-Al_2O_3-SiO_2-F_2O_{-1} (NASF)

The incorporation of fluorine in silicate systems can be rationalized as progressive fluorination, i.e. addition of F_2O_{-1}, to their chemical constituents. In order to understand fluorine behavior in felsic magmas we need to evaluate compatibilities between rock-forming silicates and solid and gaseous F-bearing phases. The

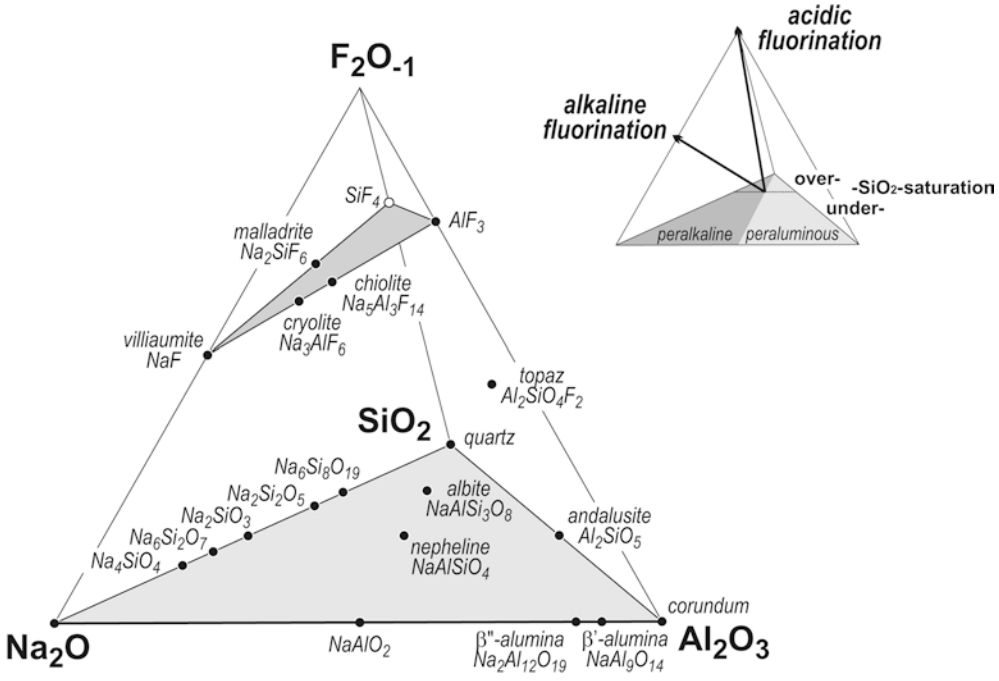

Fig. 2 Quaternary composition space of the system Na_2O-Al_2O_3-SiO_2-F_2O_{-1} with positions of rock-forming minerals, topaz and fluoride phases and petrochemical subdivisions. Symbols: *solid symbols* solid phases, *open circle* SiF_4 (g)

quaternary system Na_2O-Al_2O_3-SiO_2-F_2O_{-1} (Fig. 2) provides a good approximation for felsic magmatic systems for several reasons: (i) it contains the petrogenetically important rock-forming phases: quartz, albite and nepheline, hence it covers a wide range of $a(SiO_2)$, (ii) it extends over the full peralkaline to peraluminous compositional space, (iii) it includes the major fluoride phases, occurring in nature: villiaumite, cryolite, chiolite, malladrite, and topaz.

Fluorination reactions and mineral-gas compatibilities in the Na_2O-Al_2O_3-SiO_2-F_2O_{-1} system (cf. Anovitz et al. 1987) are computed in the temperature range 400–800 °C and at a pressure of 100 MPa to approximate suprasolidus to subsolidus conditions of shallow-crustal fluorine-bearing felsic systems. All equilibria are nearly parallel in the temperature-chemical potential section (Fig. 3), and therefore the sequence of fluorination reactions and order of occurrence of F-bearing phases are temperature independent. The relative arrangement

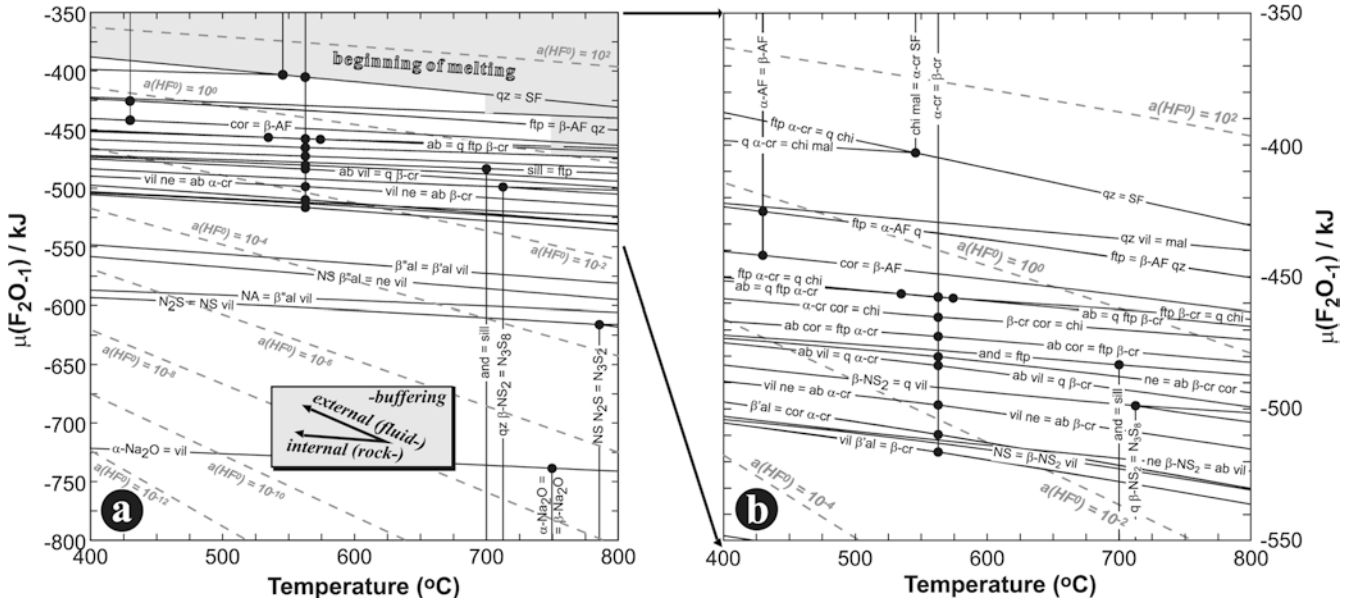

Fig. 3 Fluorination reactions in the system Na_2O-Al_2O_3-SiO_2-F_2O_{-1} at a temperature range of 400–800 °C and pressure 100 MPa: (**a**) $\mu(F_2O_{-1}) = -800$ to -350 kJ, (**b**) detail for $\mu(F_2O_{-1}) = -550$ to -350 kJ. Locations of individual equilibria are accurate to ± 7 kJ. *Gray curves* indicate activities of aqueous HF^0 (Johnson et al. 1992), defined by the equilibrium: $H_2O + [F_2O_{-1}] = 2\ HF^0$ (aq). Abbreviations: Table e1, *q* quartz, *ab* albite, *ne* nepheline, *and* andalusite, *cor* corundum

of major equilibria remains similar to that at one-atmosphere pressure (Anovitz et al. 1987) suggesting no pressure effects on the progress of fluorination.

The near-horizontal slope of equilibria implies that internal (rock-, mineral-) buffering will retain the chemical potential of F_2O_{-1} nearly constant over a large temperature range. On the contrary, isopleths of activities of HF^0,aq (proportional to molalities in the aqueous fluid phase) intersect solid-solid and solid-gas equilibria at moderate angles and shift into high $\mu(F_2O_{-1})$ with decreasing temperature. During cooling, external buffering (e.g. by pervasive fluid circulation) will progressively replace silicates by fluorides and topaz. For example, an aqueous fluid phase exsolved at 700 °C and 100 MPa from a cryolite-bearing granite will have $a(HF^0,aq) \sim 10^{-1}$ molal (Fig. 3) and will convert albite and cryolite into a chiolite-topaz-quartz rock between 480 and 400 °C.

During progressive fluorination in the Na_2O-Al_2O_3-SiO_2-F_2O_{-1} system, villiaumite appears as the first fluoride phase and is stable over a very wide range of $\mu(F_2O_{-1})$ and $a(HF^0,aq)$ (Figs. 3 and 4). The coexistence of villiaumite with alkali silicates (in order of increasing Na/Si ratio: $Na_2Si_2O_5$, Na_2SiO_3, Na_4SiO_4 etc.) buffers $\mu(F_2O_{-1})$ at decreasing levels, hence fluoride solubility in increasingly peralkaline silicate melts should decrease. Cryolite becomes stable with advancing fluorination at $\mu(F_2O_{-1}) = -519.5$ kJ, by reaction of villiaumite with sodium aluminate:

$$26\ NaF\ (villiaumite) + NaAl_9O_{14}\ (\beta'-alumina) + 14\ [F_2O_{-1}] = 9\ Na_3AlF_6\ (cryolite)$$

Villiaumite and/or cryolite remain characteristic low-$\mu(F_2O_{-1})$ phases, compatible with nepheline, albite or quartz. Topaz becomes stable at $\mu(F_2O_{-1}) = -479.3$ kJ, at the expense of andalusite:

$$Al_2SiO_5\ (andalusite) + [F_2O_{-1}] = Al_2SiO_4F_2\ (topaz)$$

Villiaumite, cryolite and topaz are the only F-bearing phases occurring in stability field of albite at $\mu(F_2O_{-1}) \leq -459.4$ kJ, i.e. they are compatible in feldspar-bearing rocks. On the contrary, high-$\mu(F_2O_{-1})$ phases—chiolite, malladrite, AlF_3 are unstable with albite and coexist with quartz only.

Chiolite forms by fluorination of corundum in the presence of cryolite at $\mu(F_2O_{-1}) = -466.5$ kJ, according to the equilibrium:

$$5\ Na_3AlF_6\ (cryolite) + 2\ Al_2O_3\ (corundum) + 6\ [F_2O_{-1}] = 3\ Na_5Al_3F_{14}\ (chiolite)$$

The formation of malladrite, according to the equilibrium:

$$2\ NaF\ (villiaumite) + SiO_2\ (quartz) + 2\ [F_2O_{-1}] = Na_2SiF_6\ (malladrite)$$

represents the upper limit of compatibility of villiaumite and quartz. The coexistence of villiaumite and quartz (e.g. Anfilogov et al. 1979; Kotelnikova and Kotelnikov 2002) indicates the range of $\mu(F_2O_{-1})$ between −494.1 and −431.1 kJ, corresponding to $a(HF^0,aq) = 10^{-1.46}$ to $10^{+0.43}$ at 600 °C and 100 MPa.

The fluorination sequence of silicates is terminated by decomposition of quartz at $\mu(F_2O_{-1}) = -408.9$ kJ, i.e. $a(HF^0,aq) = 10^{+1.09}$:

$$SiO_2\ (quartz) + 2\ [F_2O_{-1}] = SiF_4\ (g)$$

Silicon tetrafluoride exhibits a triple point at −86.7 °C and 2.24 atm and a critical point at −14.2 °C and 37 atm (Devyatykh et al. 1999) and therefore forms a non-polar supercritical fluid at elevated temperatures and pressures.

At any level of $\mu(F_2O_{-1})$, the vapor pressure of individual gaseous species is buffered by a multiphase solid assemblage through chemical potentials of thermodynamic components. SiF_4, $NaAlF_4$, NaF and $(NaF)_2$ represent the most abundant gas constituents (>99%). Within the limits of $\mu(F_2O_{-1})$ for F-bearing nepheline syenites and quartz-albite assemblages (Figs. 3 and 4), partial vapor pressures at 600 °C and 100 MPa for solids vary as follows: SiF_4 $6.27.10^{-11}$ to $9.03.10^{-4}$ bar, $NaAlF_4$ $2.10.10^{-11}$ to $1.18.10^{-6}$ bar, NaF $3.39.10^{-9}$ to $8.69.10^{-11}$ bar and $(NaF)_2$ $2.11.10^{-9}$ to $1.16.10^{-11}$ bar. Consequently, fluoride loss by vaporization is negligible and fluoride species form only an accessory fraction of gas at anhydrous conditions. In H_2O-bearing systems, HF(g) is the dominant fluoride species in low-density aqueous fluids (cf. Symonds and Reed 1993); the total vapor pressure of $(HF)_n$ ranges from $1.58.10^{-3}$ to $6.90.10^{-2}$ bar. Similarly, HF^0 and $Si(OH)_nF_{4-n}{}^0$ are major solute species in high-density aqueous fluids (Halter et al. 1998; Aksyuk and Zhukovskaya 1998; Haselton et al. 1988). Magmatic devolatilization, triggered by H_2O saturation, will likely lead to partial removal of F and Si from the melt.

Anhydrous, multiphase, fluoride-dominated assemblages at high levels of $\mu(F_2O_{-1})$ undergo partial melting. At 1-atm pressure, relevant melting points are: sodium disilicate-villiaumite eutectic (798 °C, Willgallis 1969), malladrite-villiaumite eutectic (695 °C, Chiotti 1981), cryolite-chiolite peritectic (741 °C, Foster 1970), chiolite-AlF_3 eutectic (694 °C, Foster 1970). Due to the low solubility of aluminosilicate constituents in fluoride melts (Foster 1975; Faerøyvik et al. 1999), the solidus-temperature depression of alkali fluoroaluminate and fluorosilicate melts from corresponding fluoride systems is very small (at 1-atm pressure): 16 °C for the cryolite-chiolite peritectic with addition of Al_2O_3 (Foster 1975), 15 °C for the villiaumite-cryolite eutectic with addition of nepheline (Rutlin 1998) and 13 °C for the villiaumite-fluorite eutectic with addition of nepheline (Faerøyvik et al. 1999). By using the $dT/dP \sim 14$ °C/kbar gradient for fluoride melting (Clark 1959; Pistorius 1966), the solidus boundaries are reliably located based on fluoride compatibilities (Fig. 3).

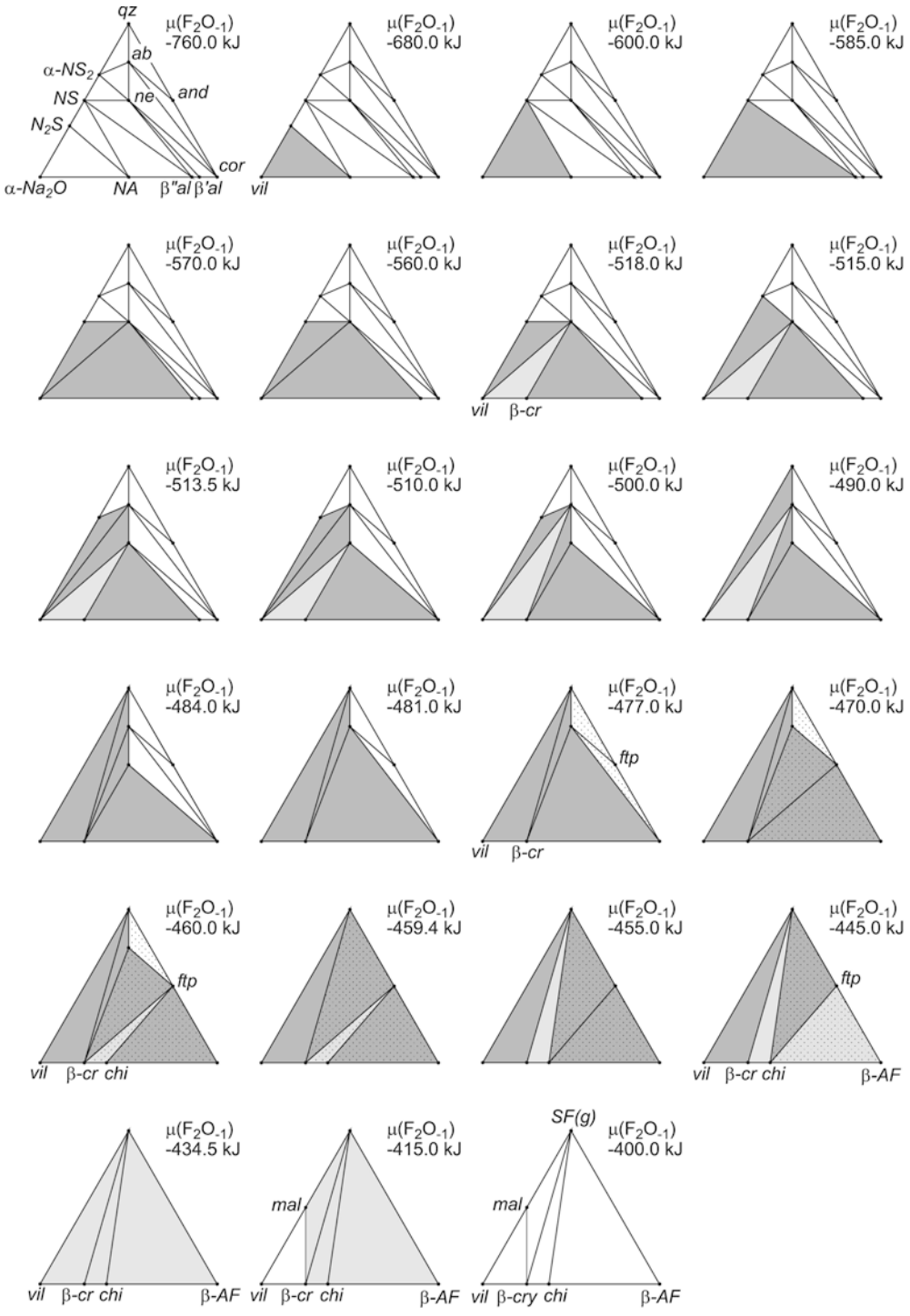

Fig. 4 Solid-gas compatibilities in the system Na_2O-Al_2O_3-SiO_2-F_2O_{-1} at 600 °C and 100 MPa, with increasing $\mu(F_2O_{-1})$ indicating fluoride/topaz-silicate compatibilities and progressive fluorination from peralkaline silica-undersaturated towards peraluminous silica-oversaturated compositions. In the H_2O-free multicomponent systems, topaz is represented by its fluorine-end member. Fill patterns: *dark gray* coexistence of one F-bearing phase with silicate phases, *light gray* coexistence of two F-bearing phases with a silicate phases, *dotted areas* coexistence of topaz with silicate or fluoride phases

Compatibilities of rock-forming minerals with F-bearing phases as well as the effects of bulk composition are presented in a series of pseudoternary diagrams (Na_2O-Al_2O_3-SiO_2), sectioned according to increasing $\mu(F_2O_{-1})$. Progressive fluorination starts at the Na_2O apex and F-bearing phases appear in the following order: villiaumite, cryolite, fluortopaz, chiolite, AlF_3, malladrite and SiF_4. Gray shadings (Fig. 4) indicate coexistence of silicates with fluoride phases and confirm the progress of fluorination from peralkaline towards peraluminous, and from silica-undersaturated towards -oversaturated bulk compositions. Consequently, peralkaline silica-undersaturated rocks will buffer fluorine concentrations in the system at the lowest levels, whereas peraluminous silica-saturated systems will attain the highest fluorine abundances.

Individual phase diagrams reveal important compatibilities (Fig. 4). Peralkaline nepheline-albite assemblages

(peralkaline nepheline syenites) are first saturated with villiaumite at $\mu(F_2O_{-1}) > -514.2$ kJ or $a(HF^0,aq) > 10^{-2.06}$:

$$2\ NaAlSiO_4\ (nepheline) + 2\ Na_2Si_2O_5 + 2\ [F_2O_{-1}] = 4\ NaF\ (villiaumite) + 2\ NaAlSi_3O_8\ (albite)$$

Villiaumite in peralkaline nepheline syenites is replaced by cryolite at $\mu(F_2O_{-1}) > -501.1$ kJ or $a(HF^0,aq) > 10^{-1.66}$, by the following equilibrium:

$$4NaF\,(villiaumite) + 3NaAlSiO_4\,(nepheline) + 4[F_2O_{-1}] = 2Na_3AlF_6\,(cryolite) + 1NaAlSi_3O_8\,(albite)$$

Peraluminous nepheline syenites remain saturated with corundum, at all levels of F_2O_{-1}. The upper stability limit for the fluorine-bearing nepheline syenites is given by the breakdown of nepheline at $\mu(F_2O_{-1}) = -482.3$ kJ or $a(HF^0,aq) = 10^{-1.10}$:

$$9\ NaAlSiO_4\ (nepheline) + 6\ [F_2O_{-1}] = 3\ NaAlSi_3O_8\ (albite) + 2\ Al_2O_3\ (corundum) + 2\ Na_3AlF_6\ (cryolite)$$

This equilibrium also limits the maximum fluorine solubility (expressed in terms of F_2O_{-1}) in silica-undersaturated magmas.

Peralkaline quartz-albite assemblages (peralkaline granites) become saturated with villiaumite at $\mu(F_2O_{-1}) > -494.1$ kJ, i.e. at higher levels than nepheline syenites. Cryolite becomes stable in granitic assemblages at $\mu(F_2O_{-1}) = -486.0$ kJ, by replacing villiaumite:

$$2\ NaF\ (villiaumite) + 1\ NaAlSi_3O_8\ (albite) + 2\ [F_2O_{-1}] = 1\ Na_3AlF_6\ (cryolite) + 3\ SiO_2\ (quartz).$$

Peraluminous granites in this system are saturated with andalusite (in the absence of ferromagnesian components), which is replaced by topaz at $\mu(F_2O_{-1}) = -479.3$ kJ:

$$1\ Al_2SiO_5\ (andalusite) + 1\ [F_2O_{-1}] = 1\ Al_2SiO_4F_2\ (topaz)$$

The occurrence of villiaumite in peralkaline silica-oversaturated rocks corresponds to significantly lower levels of F_2O_{-1} ($a(HF^0,aq) < 10^{-1.21}$) than the presence of topaz in peraluminous varieties ($a(HF^0,aq) > 10^{-1.01}$). The upper stability limit for fluorine-bearing granitic systems corresponds to the breakdown of albite at $\mu(F_2O_{-1}) = -459.4$ kJ or $a(HF^0,aq) = 10^{-0.42}$, according to the equilibrium:

$$3NaAlSi_3O_8\,(albite) + 4[F_2O_{-1}] = 1Na_3AlF_6\,(cryolite) + 1Al_2SiO_4F_2\,(topaz) + 8SiO_2\,(quartz)$$

This equilibrium converts granitic rocks (by mineralogical definition) into feldspar-free rocks. The alkali-feldspar breakdown has additional implications: (i) maximum fluorine enrichments are higher in the silica-oversaturated than in silica-undersaturated systems, and the corresponding activities of HF^0 (aq) are $10^{-1.10}$ and $10^{-0.42}$, respectively; (ii) feldspar is incompatible with "high-fluorination" phases, such as chiolite, AlF_3, malladrite or SiF_4. These phases are not stable in feldspathic rocks at near-solidus temperatures, but can form during externally buffered cooling (Fig. 3).

Because stabilities of F-bearing minerals are directly related to peralkalinity or peraluminosity of the system (Fig. 4) it is desirable to portray the fluorination of quartzofeldspathic assemblages as a function of chemical potential of Na_2O (Fig. 5), which covers the entire range of peraluminosity to peralkalinity in granitic systems. Its lower limit is given by andalusite saturation:

$$[Na_2O] + Al_2SiO_5\ (andalusite) + 5\ SiO_2\ (quartz) = 2\ NaAlSi_3O_8\ (albite)$$

The upper limit of $\mu(Na_2O)$ is related to the decomposition of quartz through the equilibrium:

$$[Na_2O] + 2\ SiO_2\ (quartz) = Na_2Si_2O_5$$

Mafic minerals (micas, amphiboles, pyroxenes, fayalite) define additional buffers, which subdivide the quartz-albite stability field (Fig. 5). Progressive fluorination is expressed as the chemical potential of F_2O_{-1}. The composition space with Na_2O and F_2O_{-1} as mobile components is limited by the saturation field of villiaumite, according to the equilibrium ($\Delta_r G = -1{,}178.9$ kJ, at 600 °C and 100 MPa):

$$[Na_2O] + [F_2O_{-1}] = 2\ NaF\ (villiaumite)$$

During magmatic differentiation crystallizing magmas will evolve along isopleths of constant $\mu(Na_2O)$ due to buffering effects of feldspars and mafic minerals, whereas fluorine compatibility in the melt (London 1997) causes $\mu(F_2O_{-1})$ to rise. At low levels of $\mu(Na_2O)$, peraluminous granites will crystallize topaz. Moderately peralkaline granites (as indicated by the presence of riebeckite) will precipitate cryolite, and strongly peralkaline granites (with aegirine) saturate with cryolite or villiaumite.

Major hydrothermal alteration styles—greisenization, albitization and alkali metasomatism follow orthogonal trends in terms of $\mu(F_2O_{-1})$ and $\mu(Na_2O)$. Greisenization is characterized by concomitant hydrolysis and fluorination (Burt 1974; Štemprok 1987), leading to progressive destabilization of feldspars (topaz-quartz greisens) and aluminosilicates (quartz greisens). Hydrothermal albitization (e.g. Barton et al. 1991) of topaz-bearing granites only requires an increase in $\mu(Na_2O)$ at constant $\mu(F_2O_{-1})$ and will be followed by cryolitization. Whereas mobility of F_2O_{-1} and Na_2O produces distinct alteration products in peraluminous systems and can provide additional information on fluid characteristics, the addition either of F_2O_{-1} or Na_2O to peralkaline systems will only lead to cryolitization.

These equilibria are topologically similar to those in the μ(HF)-μ(NaF) coordinate space (Burt and London

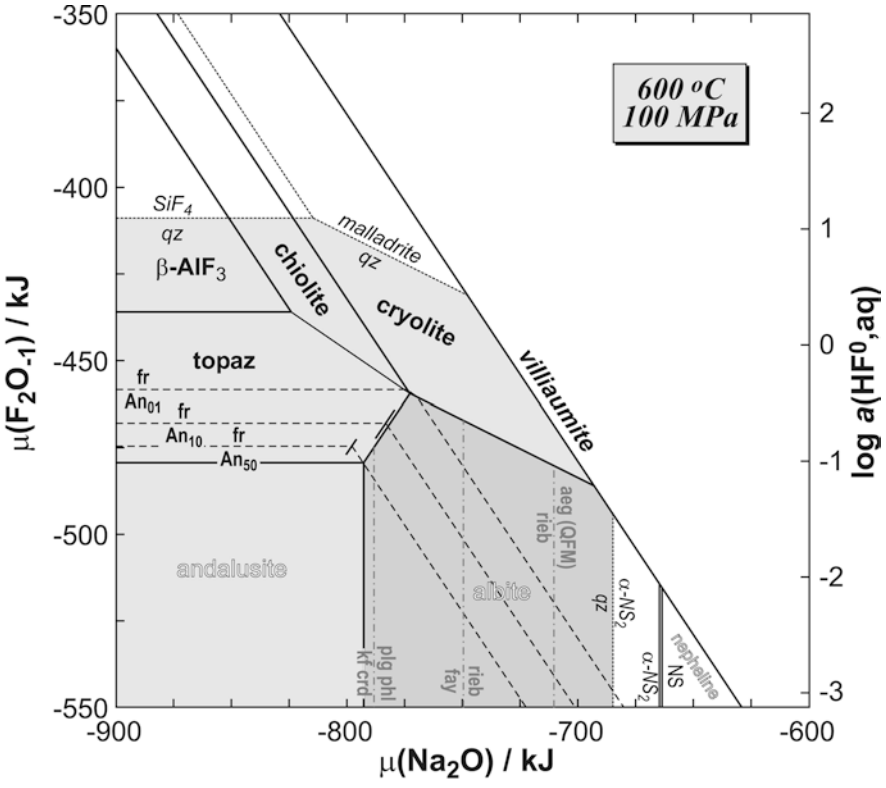

Fig. 5 $\mu(Na_2O)$ *vs.* $\mu(F_2O_{-1})$ diagram of the system Na_2O-Al_2O_3-SiO_2-F_2O_{-1} at 600°C and 100 MPa. *Light gray field* indicates the presence of quartz; *dark gray field* corresponds to quartz + albite assemblage. *Black dashed lines* are contours of fluorite saturation in the Ca-bearing system as function of plagioclase composition. Bulk composition: SiO_2 : Al_2O_3 = 10:1 molar, mobile components: Na_2O, F_2O_{-1}. Additional abbreviations: *aeg* aegirine, *crd* cordierite, *fay* fayalite, *kf* K-feldspar, *phl* phlogopite, *plg* plagioclase, *rieb* riebeckite, and *QFM* quartz-fayalite-magnetite buffer

1982). Phases $NaHF_2$ (s), ralstonite and rosenbergitee are unstable at high-temperature hydrothermal and near-solidus conditions; $NaHF_2$ decomposes into HF and villiaumite between 270–278 °C (von Wartenberg and Bosse 1922; Froning et al. 1947), ralstonite dehydrates at 302 °C (Ryabenko et al. 1988) and rosenbergite undergoes stepwise dehydration between 125 and 320 °C (Grobelny 1977; Menz et al. 1988).

Addition of CaO to the system Na_2O-Al_2O_3-SiO_2-F_2O_{-1} will cause saturation with fluorite and severely limit the fluorine enrichment, particularly in peralkaline granites. In peralkaline and metaluminous environments, fluorite saturation is related to decalcification of plagioclase:

$$CaAl_2Si_2O_8\,(\text{plagioclase}) + 4\,SiO_2\,(\text{quartz}) + [Na_2O] + [F_2O_{-1}] = CaF_2\,(\text{fluorite}) + 2\,NaAlSi_3O_8\,(\text{plagioclase})$$

In peraluminous compositions, fluorite saturation occurs by concomitant formation of topaz:

$$CaAl_2Si_2O_8\,(\text{plagioclase}) + 2\,[F_2O_{-1}] = CaF_2\,(\text{fluorite}) + Al_2SiO_4F_2\,(\text{topaz}) + SiO_2\,(\text{quartz})$$

These equilibria are divariant in the Na_2O vs. F_2O_{-1} composition space due to continuous solid-solution changes, i.e. decalcification (albitization) of plagioclase. Since saturation with fluorite always occurs at lower $\mu(F_2O_{-1})$ than the formation of cryolite or villiaumite (Figs. 5 and 6), peralkaline granite magmas with Ca-bearing plagioclase will crystallize fluorite and do not reach saturation with cryolite or villiaumite, unless plagioclase has been converted into nearly pure albite.

Addition of K_2O represents an extension towards the complete haplogranite system and portrays alteration equilibria in greisen environments (Burt 1981). The important difference are: (i) the stability of quartz is more restricted due to the presence of $K_2Si_4O_9$; consequently, carobbiite is not compatible with quartz and is not stable in granitic suites. (ii) the K-feldspar—K_3AlF_6 equilibrium is shifted to higher levels of $\mu(F_2O_{-1})$ than the albite—cryolite equilibrium. Therefore, peralkaline granites will precipitate cryolite, and K_3AlF_6 will not form until albitic feldspar has been completely converted into cryolite. This sequence is in agreement with the abundance of alkali aluminofluorides in natural conditions: cryolite is the most common aluminofluoride (Pauly 1960; Korytov et al. 1984; Horbe et al. 1991), elpasolite KNa_2AlF_6 is a minor phase rarely found in F-rich granitic pegmatites (Bailey 1980), and K_3AlF_6 has not yet been identified as a natural mineral.

Phase equilibria in the system CaO-Al_2O_3-SiO_2-F_2O_{-1} (CASF)

Fluorite, CaF_2, is one of the most common accessory minerals in calc-alkaline and peralkaline silicic magmas (Marshall et al. 1998; Price et al. 1999; Webster and Rebbert 2001), associated skarns (Burt 1972), and high-grade quartzofeldspathic gneisses (Bohlen and Essene

1978). The fluorite stability in magmas is controlled by the equilibrium:

$$[CaO] + [F_2O_{-1}] = CaF_2$$

Hence, activities of CaO and F_2O_{-1} exert reciprocal effects on the fluorite saturation. The lower limit of μ(CaO) is determined by saturation with aluminosilicate

$$[CaO] + Al_2SiO_5\ (\text{andalusite}) + SiO_2\ (\text{quartz}) = CaAl_2Si_2O_8\ (\text{plagioclase})$$

demonstrating the relationship between μ(CaO), melt peraluminosity and plagioclase composition. The upper limit of μ(CaO) is given by the stability of wollastonite:

$$[CaO] + SiO_2\ (\text{quartz}) = CaSiO_3\ (\text{wollastonite})$$

Natural multicomponent systems provide many additional buffers of μ(CaO): enstatite—actinolite (Ca-amphibole) - diopside, phlogopite—actinolite (amphibole) / K-feldspar, rutile—titanite, and ilmenite—titanite / magnetite. In Fig. 6, all amphibole-, clinopyroxene- or titanite-bearing magmas saturate with fluorite. Fluorite buffers fluorine concentration in the melt (or a fluid) at decreasing levels ($\mu(F_2O_{-1}) < -470$ kJ) with increasing μ(CaO). Low-Ca or peraluminous magmas saturate with topaz at higher fluorine concentrations, $\mu(F_2O_{-1}) > -480$ kJ. Cryolite stability is restricted to extremely Ca-poor compositions ($An_{<01}$). The maximum (buffered) solubility of fluorine is determined by the low-variance equilibria, in Ca-rich and Ca-poor granitic melts, respectively:

$$CaAl_2Si_2O_8\ (\text{plagioclase}) + 2\ [F_2O_{-1}] = Al_2SiO_4F_2\ (\text{topaz}) + CaF_2\ (\text{fluorite}) + SiO_2\ (\text{quartz})$$

$$3\,NaAlSi_3O_8\,(\text{plagioclase}) + 4\,[F_2O_{-1}] = Na_3AlF_6\,(\text{cryolite}) + Al_2SiO_4F_2\,(\text{topaz}) + 8\,SiO_2\,(\text{quartz})$$

Effects of plagioclase composition, peralkalinity and silica saturation

The major-element variation of natural felsic magmas spans the Na_2O-K_2O-CaO-Al_2O_3-SiO_2 system and can be completely described by three independent variables: silica saturation, peralkalinity, and feldspar composition. These factors were historically incorporated in the alumina saturation index (Shand 1927), the alkali-lime index (Peacock 1931), and the silica saturation concept (Carmichael et al. 1970). Relationships between compositional and thermodynamic parameters have been introduced by studies on silica activity in natural magmas (Carmichael et al. 1970), followed by Barton et al.'s (1991) and Barton's (1996) descriptions of composition space of felsic magmas by using $a(SiO_2)$, $a(Al_2O_3)$ and a(CaO). At arbitrary P and T compositional parameters

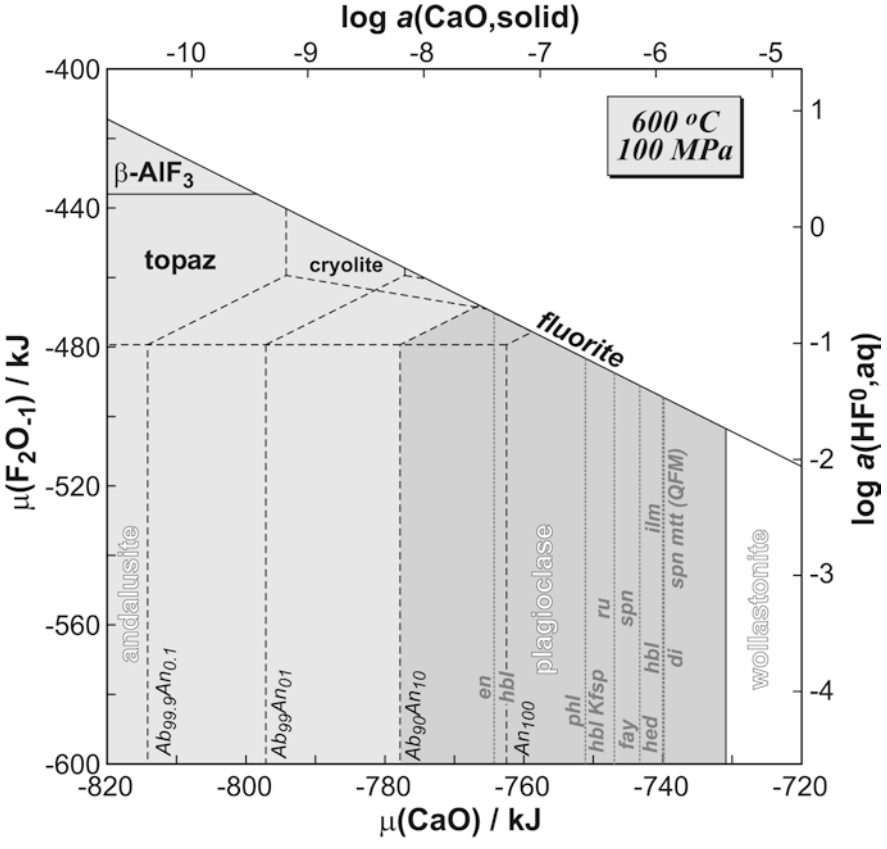

Fig. 6 μ(CaO) vs. $\mu(F_2O_{-1})$ projection of the system Na_2O-CaO-Al_2O_3-SiO_2-F_2O_{-1} at 600 °C, 100 MPa and quartz saturation. *Light gray field* indicates the presence of the assemblage albite + quartz; *dark gray field* corresponds to the plagioclase (An_{10}) + quartz assemblage. Notice shrinking of andalusite and topaz stability fields with decreasing An-content of plagioclase and closing of cryolite stability field at $An_{>3}$. Additional abbreviations: *di* diopside, *en* enstatite, *hbl* hornblende, *ilm* ilmenite, *mtt* magnetite, *ru* rutile, *spn* titanite

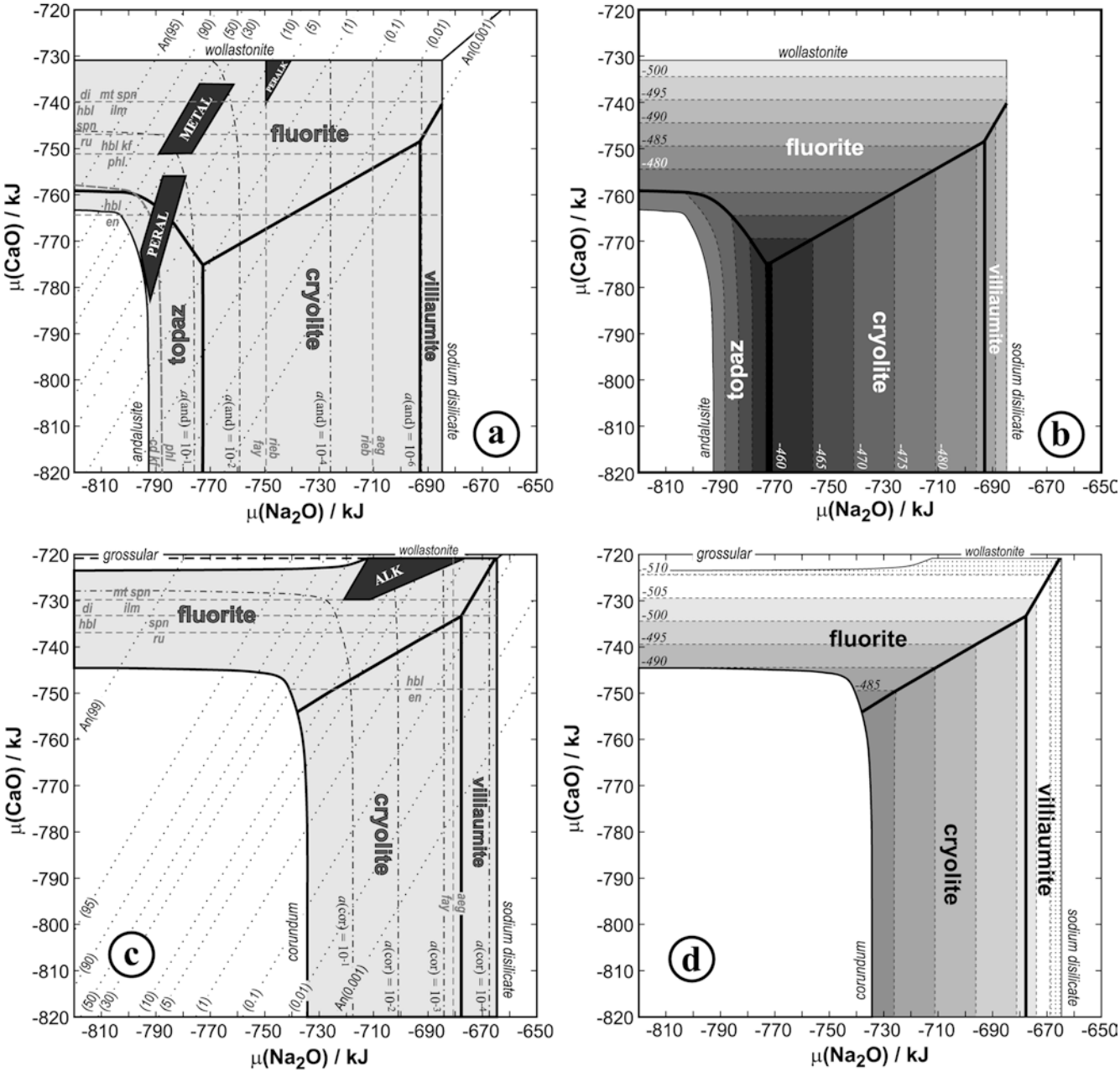

Fig. 7 $\mu(Na_2O)$ vs. $\mu(CaO)$ projection of the system Na_2O-CaO-Al_2O_3-SiO_2-F_2O_{-1} at 600 °C and 100 MPa illustrating compatibilities between granitic or nepheline-syenitic rock types and F-bearing minerals: **a** $a(SiO_2) = 1$, i.e. at quartz saturation. Chemical potentials of Na_2O and CaO are related through plagioclase equilibrium (*dotted lines*): $[CaO] + 2\ NaAlSi_3O_8\ (ss) = [Na_2O] + CaAl_2Si_2O_8\ (ss) + 4\ SiO_2\ (s)$ and that of F_2O_{-1} by the coexistence of quartz, plagioclase and the fluoride phase. Abbreviations for rock groups: *PERAL* peraluminous granites, *METAL* metaluminous granodiorites to tonalities, *PERALK* peralkaline granites. **b** $a(SiO_2) = 1$, isopleths of $\mu(F_2O_{-1})$ in kJ at quartz, plagioclase and F-bearing phase equilibrium. **c** $a(SiO_2) = 0.25$, i.e. at nepheline-albite equilibrium. Abbreviation for rock group: *ALK* alkaline nepheline syenites. **d** $a(SiO_2) = 0.25$, isopleths of $\mu(F_2O_{-1})$ in kJ at nepheline, plagioclase and fluoride phase equilibrium

of any felsic rock: melt peralkalinity, peraluminosity and chemical potentials of system constituents are directly related to feldspar composition:

$$[CaO] + [Al_2SiO_5] + SiO_2\ (\text{quartz}) = CaAl_2Si_2O_8\ (\text{plagioclase})$$

$$[Na_2O] + [Al_2SiO_5] + 5\ SiO_2\ (\text{quartz}) = 2\ NaAlSi_3O_8\ (\text{plagioclase})$$

Therefore and in the common absence of K-bearing fluoride phases, only two independent variables at constant $a(SiO_2)$ provide a complete description of the composition space of felsic rocks as well as compatibilites of F-bearing phases in the system Na_2O-CaO-Al_2O_3-SiO_2-F_2O_{-1}. In this discussion, $\mu(Na_2O)$ and $\mu(CaO)$ are used as independent variables at constant $a(SiO_2)$, and plagioclase composition, melt peraluminosity as well as the position of various solid-solid buffers are plotted in this thermodynamic frame. F_2O_{-1}

is treated as a thermodynamically immobile component buffered by the coexistence of plagioclase with a F-bearing phase at constant $a(SiO_2)$, hence the calculation of equilibria in this system does not require bulk composition constraints.

The composition space of felsic rocks is limited by the conversion of quartz, nepheline or plagioclase into aluminous (andalusite, corundum), alkaline (sodium silicate) or Ca-rich phases (wollastonite, grossular). Further subdivisions are provided by mafic-silicate and oxide buffers (Fig. 7, cf. Figs. 5 and 6). In granitic rocks with $a(SiO_2)$ near unity, saturation with topaz, fluorite, cryolite or villaumite is controlled by the plagioclase composition and system peralkalinity (peraluminosity) (Fig. 7a). Villiaumite is stable in extremely peralkaline conditions: $\mu(Na_2O) > -693$ kJ, coexisting with pure albite ($An_{<0.001}$) only. Similarly, cryolite stability requires the coexistence with pure albite ($An_{<02}$) and occurs in Ca-poor environments. Natural granitic rocks with Ca-bearing plagioclase ($An_{>05}$) saturate with topaz or fluorite. The stability of topaz is restricted to peraluminous conditions at $a(Al_2SiO_5)$ greater than approximately 10^{-1} (Fig. 7a), consistent with the presence of Li-micas or anhydrous aluminosilicates (cordierite, garnet, andalusite). Fluorite crystallization is limited to high-Ca/Na environments and it becomes a saturating fluoride in peraluminous biotite granites, amphibole, clinopyroxene or titanite-bearing calc-alkaline suites as well as in peralkaline granitic rocks (Fig. 7a).

Highly variable levels of fluorine enrichment observed in natural magmas (0.2 to ~8 wt%, Fig. 1) are depicted by the shape of $\mu(F_2O_{-1})$ surface at the feldspar/F-bearing phase-saturating interface (Fig. 7b). The lowest levels of fluorine concentration are attained at Ca-rich or strongly peralkaline environments with $\mu(F_2O_{-1}) < -490$ kJ. The chemical potential of $\mu(F_2O_{-1})$ increases towards low-Ca and peraluminous conditions and reaches its maximum at the cryolite, topaz, fluorite invariant point at $\mu(F_2O_{-1}) = -459$ kJ. Consequently, villiaumite-saturated magmas will strongly inhibit fluorine enrichment, whereas low-Ca topaz- or cryolite-bearing melts will achieve the highest fluorine concentrations. Similarly, the levels of maximum increase in fluorine solubility increase from peralkaline through metaluminous to peraluminous conditions. The variation range of ~60 kJ $\mu(F_2O_{-1})$ corresponds to 1.5 log units of $a(HF^0, aq)$. These results are also consistent with natural observations on fluorine melt concentrations increasing from evolved peralkaline rhyolites (maximum 1.5 wt% F; Webster and Rebbert 2001) towards peraluminous topaz-bearing ongonites (maximum 3.5 wt% F; Kovalenko and Kovalenko 1984; Štemprok 1991).

The effect of silica activity provides an explanation for the strong difference in fluorine melt-inclusion contents in granites vs. nepheline syenites (Fig. 1). Fig. 7c provides comparative phase diagrams at $a(SiO_2) = 0.25$, as buffered by nepheline-albite equilibrium. The large

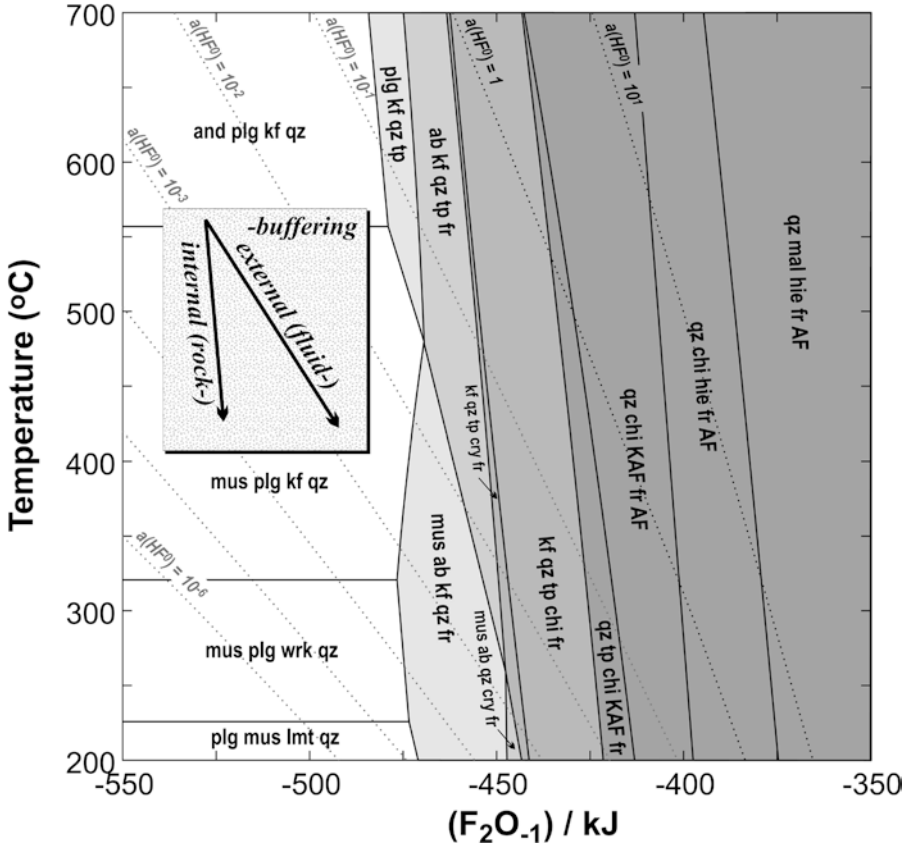

Fig. 8 Temperature–$\mu(F_2O_{-1})$ pseudosection in the system qz-kf-ab-an-Al_2O_3-F_2O_{-1} at 100 MPa and quartz and H_2O saturation showing subsolidus evolution of fluorogranitic systems during internally and externally buffered conditions. *Gray shading* indicates stability of one, two, three or four F-bearing phases, respectively. Bulk composition (at quartz and H_2O saturation): $Ab_{54}Or_{36}An_{10}$ (A/CNK = 1.2). Alkali feldspar and topaz are solid solutions (Wen and Nekvasil 1994; Barton 1982). Additional abbreviations: *fsp* feldspar, *lmt* laumontite, *wrk* wairakite

stability field of corundum severely restricts the potential for high $\mu(F_2O_{-1})$ levels and eliminates the occurrence of topaz in silica-undersaturated rocks. The cryolite stability field slightly expands with decreasing activity of silica at the expense of villiaumite and fluorite, due to the equilibria:

$$6\ NaF\ (villiaumite) + NaAlSi_3O_8\ (plagioclase) = Na_3AlF_6\ (cryolite) + 2\ [Na_2O] + 3\ SiO_2$$

$$3\ CaF_2\ (fluorite) + 7\ NaAlSi_3O_8\ (plagioclase) = Na_3AlF_6\ (cryolite) + 3\ CaAl_2Si_2O_8\ (plagioclase) + 2\ [Na_2O] + 15\ [SiO_2]$$

Corundum-bearing nepheline syenites have the highest potential for fluorine enrichment before they reach cryolite saturation. Titanite-bearing nepheline-syenite magmas achieve very low fluorine concentrations by saturating with fluorite at $\mu(F_2O_{-1}) < -505$ kJ, which is 10 to 50 kJ lower than in granitic rocks. These results favourably compare with lower fluorine concentrations in melt inclusions from evolved nepheline syenites than in those from evolved granitic rocks (e.g. Harms and Schmincke 2000, Fig. 1).

Solidus and hydrothermal equilibria in F-bearing granitic systems

Granitic melts achieve the highest fluorine enrichments among all igneous suites (Figs. 1 and 7) and are often associated with prominent alteration aureoles (Pollard et al. 1987; Barton et al. 1991), e.g. greisenization (Štemprok 1987), alkali feldspatization (Charoy and Pollard 1989) or cryolitization (Horbe et al. 1991; Kovalenko et al. 1995). We investigate the effects of fluorination and temperature on several representative bulk compositions, covering metaluminous to peraluminous and Ca-free to Ca-bearing granitic compositions. A representative phase diagram for a peraluminous Ca-bearing granite is presented in Fig. 8.

With increasing $\mu(F_2O_{-1})$, quartzofeldspathic assemblages are converted into topaz, cryolite, fluorite and other fluoride phases. In Ca-free environments, subaluminous granitic rocks are buffered by topaz and cryolite, over a wide temperature range of 700–250 °C:

$$3\ NaAlSi_3O_8\ (albite) + 4\ [F_2O_{-1}] = 1\ Na_3AlF_6\ (cryolite) + 1\ Al_2SiO_4F_2\ (topaz) + 8\ SiO_2\ (quartz)$$

In peraluminous suites, the levels of fluorine enrichment are buffered by the andalusite- or muscovite–topaz equilibria (above or below 555 °C, respectively):

$$Al_2SiO_5\ (andalusite) + [F_2O_{-1}] = Al_2SiO_4F_2\ (topaz)$$

$$KAl_3Si_3O_{10}(OH)_2(muscovite) + SiO_2(quartz) + [F_2O_{-1}] = Al_2SiO_4F_2(topaz) + KAlSi_3O_8(K-feldspar) + H_2O$$

The addition of CaO to the haplogranite system implies the potential stability of fluorite as well as involvement of Ca-bearing plagioclase in the solid-state equilibria (Fig. 8). Metaluminous granitic suites become co-saturated with fluorite and topaz above 475 °C, with simultaneous decalcification of plagioclase:

$$CaAl_2Si_2O_8\ (plagioclase) + 2\ [F_2O_{-1}] = Al_2SiO_4F_2\ (topaz) + CaF_2\ (fluorite) + SiO_2\ (quartz)$$

In peraluminous Ca-bearing granites saturation with topaz precedes that of fluorite by andalusite or muscovite breakdown:

$$Al_2SiO_5\ (andalusite) + [F_2O_{-1}] = Al_2SiO_4F_2\ (topaz)$$

$$KAl_3Si_3O_{10}(OH)_2\ (muscovite) + SiO_2\ (quartz) + [F_2O_{-1}] = Al_2SiO_4F_2\ (topaz) + KAlSi_3O_8\ (K-feldspar) + H_2O$$

Below 475°C, topaz becomes unstable in all Ca-bearing suites and the formation of fluorite involves K-feldspar and muscovite:

$$CaAl_2Si_2O_8\ (plagioclase) + KAlSi_3O_8\ (K-feldspar) + [F_2O_{-1}] + H_2O = KAl_3Si_3O_{10}(OH)_2\ (muscovite) + CaF_2\ (fluorite) + 2\ SiO_2\ (quartz)$$

The fluorine concentrations in the silicate melt or the aqueous fluid will be internally buffered by the presence of feldspars at the stability limit of the first or the first two simultaneous F-bearing phases. Progressive fluorination, i.e. increasing $\mu(F_2O_{-1})$, leads to the decomposition of feldspars and micas and produces the following sequence of phases: chiolite, K_3AlF_6, AlF_3, hieratite and malladrite (Fig. 8). The subparallel course of the stability boundaries indicates that temperature does not have a significant effect on the mutual stabilities and compatibilities between rock-forming silicates and these "high-fluorination" phases.

The oblique intersections of isopleths of $a(HF^0, aq)$ with phase boundaries implies that a rock-buffered fluid phase will have progressively lower fluorine concentrations with decreasing temperature. On the other hand, the externally buffered alteration path (e.g. percolation of high-temperature magmatic fluids) will lead to progressive fluorination with decreasing temperature, i.e. breakdown of feldspars, topaz and coexistence of chiolite, K_3AlF_6, AlF_3, hieratite and malladrite with quartz (Fig. 8).

The first saturating F-bearing phase appears related to mica-feldspar low-temperature equilibria. Since the fluorine concentrations in a silicate melt or a hydrothermal fluid are buffered by the first F-bearing phase (stable with feldspar and mica), it is necessary to investigate these equilibria in more detail.

The instability of feldspars and occurrence of hydrothermal fluorite in greisen deposits (e.g. Burt 1981; Štemprok 1987) prompts evaluation of feldspar-mica-quartz-fluorite equilibria in peraluminous environments with decreasing temperature. Barton (1982) and Haapala (1997) proposed an origin of fluorite by subsolidus decalcification of magmatic plagioclase and/or K-feldspar breakdown:

$$CaAl_2Si_2O_8\,(plagioclase)+4HF\,(aq)=Al_2SiO_4F_2\,(topaz)+CaF_2\,(fluorite)+SiO_2\,(quartz)+2H_2O$$

$$CaAl_2Si_2O_8\ (plagioclase)+KAlSi_3O_8\ (K-feldspar)+2\ HF\ (aq)=KAl_3Si_3O_{10}(OH)_2\ (muscovite)+CaF_2\ (fluorite)+2\ SiO_2\ (quartz)$$

$$CaAl_2Si_2O_8\,(plagioclase)+2KAlSi_3O_8\,(K-feldspar)+Al_2SiO_4F_2\,(topaz)+2H_2O=2KAl_3Si_3O_{10}(OH)_2\,(muscovite)+CaF_2\,(fluorite)+3SiO_2\,(quartz)$$

These equilibria require open-system fluorination, i.e. subsolidus interaction of HF-bearing aqueous fluid phase with solid granites. However, we demonstrate that topaz, fluorite and cryolite undergo mutual transformations in the closed system and their presence provides valuable information on equilibrium temperatures. Fig. 9 illustrates a temperature-composition pseudosection for the system Ca-bearing granite—topaz (at H_2O saturation) to depict subsolidus closed-system equilibria of topaz-bearing granites (isoplethic path) and effects of hydrolytic alteration, i.e. alkali leaching during greisenization (non-isoplethic path). At near-solidus conditions (above 600 °C), quartz, K-feldspar, plagioclase and topaz are the stable mineral assemblage, representing Ca-bearing topaz granites. With decreasing temperature, the F-topaz end-member becomes unstable (cf. Barton 1982), causing enrichment of topaz solid solution in hydroxyl end-member; the released fluorine is incorporated in fluorite by decalcification of plagioclase:

$$CaAl_2Si_2O_8\,(plagioclase)+Al_2SiO_4F_2\,(topaz)+2H_2O=CaF_2\,(fluorite)+2Al_2SiO_4(OH)_2\,(topaz)+SiO_2\,(quartz)$$

Depending on the initial topaz F/(F + OH) ratio fluorite forms by this subsolidus reaction below approximately 600 °C in topaz-bearing granites. With decreasing temperature, the formation of white mica requires destabilization of feldspar *and* an aluminosilicate phase (i.e. topaz). This divariant transformation is bracketed by the following equilibria:

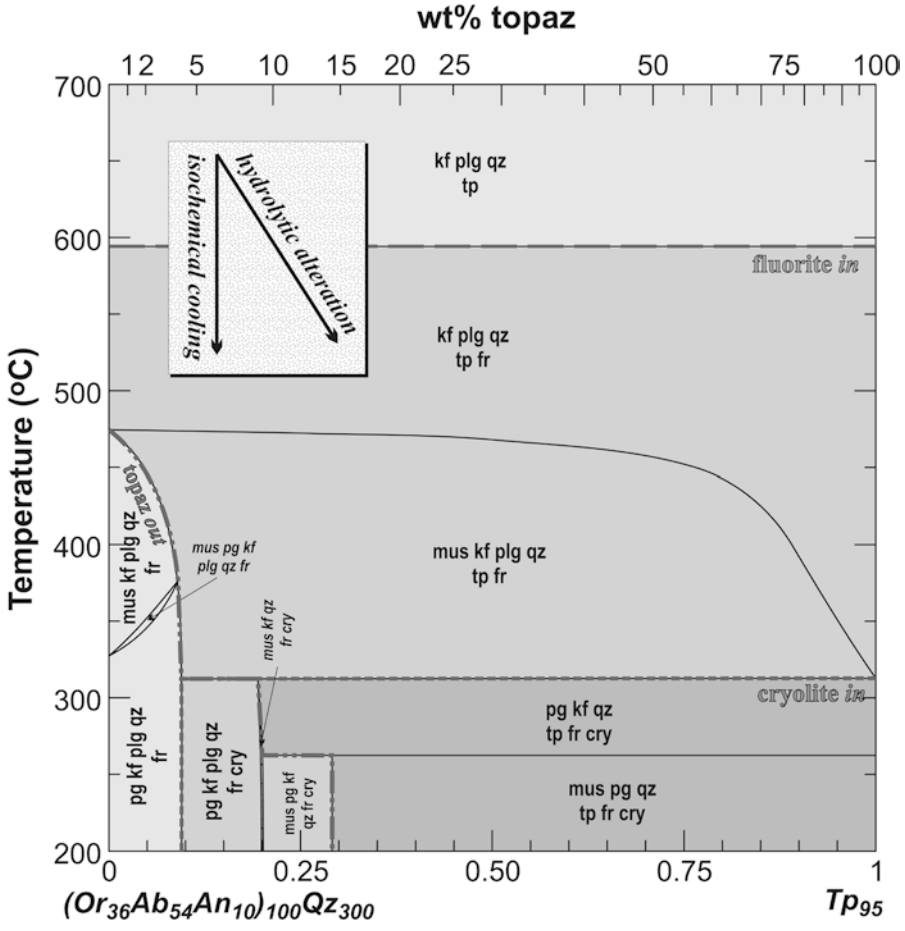

Fig. 9 Temperature–composition pseudosection for the haplogranodiorite-topaz system at 100 MPa and H_2O saturation illustrating the fluoride-topaz-feldspar-mica equilibria during isochemical subsolidus cooling (*vertical trend*) and hydrolytic alteration (*oblique trend*). *Gray shading* indicates stability of one, two or three F-bearing phases, respectively. Alkali feldspar, white mica and topaz are solid solutions (Wen and Nekvasil 1994; Chatterjee and Froese 1975; Barton 1982). Additional abbreviations: *pg* paragonite

$$Al_2SiO_4(OH)_2\ (\text{topaz}) + KAlSi_3O_8\ (\text{feldspar}) = KAl_3Si_3O_{10}(OH)_2\ (\text{muscovite}) + SiO_2\ (\text{quartz})$$

$$CaAl_2Si_2O_8\ (\text{plagioclase}) + KAlSi_3O_8\ (K-\text{feldspar}) + Al_2SiO_4F_2\ (\text{topaz}) + 2\ H_2O = 2\ KAl_3Si_3O_{10}(OH)_2\ (\text{muscovite}) + CaF_2\ (\text{fluorite}) + 3\ SiO_2\ (\text{quartz})$$

These reactions lead to further consumption of topaz and converge to an invariant point at 0 wt% topaz and T = 475 °C. The assemblage of quartz, plagioclase, K-feldspar, topaz, secondary muscovite and secondary fluorite between 475 and 315 °C corresponds to muscovitized topaz-albite granites (e.g. Ryabchikov et al. 1996; Dolejš and Štemprok 2001). In initially low-topaz (< 4 wt%) protoliths the above equilibria will lead to complete replacement of topaz by muscovite and fluorite. The appearance of cryolite at low temperatures (< 315 °C) is associated with conversion of albite into paragonite:

$$7\,NaAlSi_3O_8\ (\text{plagioclase}) + 3\,Al_2SiO_4F_2\ (\text{topaz}) + 4\,H_2O = 1\,Na_3AlF_6\ (\text{cryolite}) + 4\,NaAl_3Si_3O_{10}(OH)_2\ (\text{Na-mica}) + 12\,SiO_2\ (\text{quartz})$$

This reaction proceeds until complete consumption of topaz (for initial contents 4–10 wt% topaz) or plagioclase (initially more than 10 wt% topaz). The low-temperature stable assemblages contain up to three F-bearing phases—fluorite, cryolite and topaz, in addition to Na-mica, K-mica and quartz (Fig. 9). The relatively high temperatures of greisen formation (350–450 °C, Witt 1988; Halter et al. 1996), however, explain the relative paucity of these alteration assemblages in nature. In summary, these results suggest the absence of magmatic fluorite in Ca-bearing topaz granitic rocks. During subsolidus conditions, several modes of fluorite formation: (i) closed-system defluorination of topaz, (ii) open-system decalcification of plagioclase or (iii) hydrolytic alteration explain its abundance in granitic plutons and their hydrothermal aureoles.

Acknowledgements This study represents part of the senior author's Ph.D. thesis, supported by the J. B. Lynch and Carl Reinhardt Fellowships from McGill University. The research was supported by grants from the Natural Sciences and Engineering Research Council of Canada to D.R.B. Computation of phase diagrams was enhanced by use of Perplex (Connolly and Petrini 2002) and Theriak codes (de Capitani and Brown 1987). We would like to acknowledge discussions with Miroslav Štemprok and Jamie Connolly as well as critical reviews by Jim Webster and Donald Burt, which helped to improve the manuscript.

References

Aksyuk AM (1995) Estimation of fluorine concentrations in fluids of mineralized skarn systems. Econ Geol 95:1339–1347

Aksyuk AM, Zhukovskaya TN (1998) The solubility of quartz in aqueous solutions of hydrofluoric acid at temperatures of 500–1,000 °C and pressures of 100–500 MPa. Dokl Earth Sci 361:745–748

Anderson JL (1996) Status of thermobarometry in granitic batholiths. Trans R Soc Edinb: Earth Sci 87:125–138

Anderson GM, Castet S, Schott J, Mesmer RE (1991) The density model for estimation of thermodynamic parameters of reactions at high temperatures and pressures. Geochim Cosmochim Acta 55:1769–1779

Anfilogov VN, Bragina GI, Bobylev IB, Zyuzeva NA (1979) Structural position of fluorine and chlorine in a silicate melt. Geochem Int 16:17–22

Anovitz LM, Hemingway BS, Westrum EF jr, Metz GW, Essene EJ (1987) Heat capacity measurements for cryolite (Na_3AlF_6) and reactions in the system Na-Fe-Al-Si-O-F. Geochim Cosmochim Acta 51:3087–3103

Bailey JC (1977) Fluorine in granitic rocks and melts: a review. Chem Geol 19:245–256

Bailey JC (1980) Formation of cryolite and other aluminofluorides: a petrologic review. Bull Geol Soc Den 29:1–45

Bale CW, Chartrand P, Degterov SA, Eriksson G, Hack K, Ben Mahfoud R, Melançon J, Pelton AD, Petersen S (2002) FactSage thermochemical software and databases. CALPHAD 26:189–228

Barin I (1993) Thermochemical data of pure substances. VCH, New York, 1739 pp

Barton MD (1982) The thermodynamic properties of topaz solid solutions and some petrologic applications. Am Mineral 67:956–974

Barton MD (1996) Granitic magmatism and metallogeny of southwestern North America. Geol Soc Am Spec Pap 315:261–280

Barton MD, Haselton HT jr, Hemingway BS, Kleppa OJ, Robie RA (1982) The thermodynamic properties of fluor-topaz. Am Mineral 67:350–355

Barton MD, Ilchik RP, Marikos MA (1991) Metasomatism. Rev Mineral 26:321–350

Berman RG (1988) Internally consistent thermodynamic data for minerals in the system Na_2O-K_2O-CaO-MgO-FeO-Fe_2O_3-Al_2O_3-SiO_2-TiO_2-H_2O-CO_2. J Petrol 29:445–522

Bohlen SR, Essene EJ (1978) The significance of metamorphic fluorite in Adirondacks. Geochim Cosmochim Acta 42:1669–1678

Burt DM (1972) The influence of fluorine on the facies of Ca-Fe-Si skarns. Carnegie Inst Wash Year Book 71:443–449

Burt DM (1974) Concepts of acidity and basicity in petrology—the exchange operator approach. Geol Soc Am Abstr Progr 6:674–676

Burt DM (1976a) Hydrolysis equilibria in the system K_2O-Al_2O_3-SiO_2-H_2O-Cl_2O_{-1}: comments on topology. Econ Geol 71:665–671

Burt DM (1976b) Generation of high HF fugacities in miarolitic pegmatites and granites: the possible role of topaz. Geol Soc Am Abstr Progr 8:798

Burt DM (1979) Geometrical analysis of cryolite and related mineral stabilities in the system Na_2O-Al_2O_3-SiO_2-F_2O_{-1}. EOS Trans Am Geophys Union 60:965

Burt DM (1981) Acidity-salinity diagrams—application to greisen and porphyry deposits. Econ Geol 76:832–843

Burt DM, London D (1982) Subsolidus equilibria. In Černý P (ed) Granitic pegmatites in science and industry. Min Assoc Can Short Course 8:329–346

Candela PA (1990) Theoretical constraints on the chemistry of the magmatic aqueous phase. Geol Soc Am Spec Pap 246:11–20

Carmichael ISE, Nicholls J, Smith AL (1970) Silica activity in igneous rocks. Am Mineral 55:246–263

Charoy B, Pollard PJ (1989) Albite-rich, silica-depleted metasomatic rocks at Emuford, northeast Queensland: mineralogical, geochemical, and fluid inclusion constraints on hydrothermal evolution and tin mineralization. Econ Geol 84:1850–1874

Chartrand P, Pelton AD (2001) Thermodynamic evaluation and optimization of the LiF-NaF-KF-MgF_2-CaF_2 system using the modified quasichemical model. Metall Mater Trans 32A:1385–1396

Chase MW (1998) (ed) NIST-JANAF thermochemical tables. J Phys Chem Ref Data, Monogr 9

Chatterjee ND, Froese E (1975) Thermodynamic study of the pseudobinary join muscovite-paragonite in the system $KAlSi_3O_8$-$NaAlSi_3O_8$-Al_2O_3-SiO_2-H_2O. Am Mineral 60:985–993

Chiotti P (1981) The pseudobinary system NaF-Na_2SiF_6. J Less-Common Metals 80:105–113

Clark SP Jr (1959) Effect of pressure on the melting points of eight alkali halides. J Chem Phys 31:1526–1531

Connolly JAD, Petrini K (2002) An automated strategy for calculation of phase diagram sections and retrieval of rock properties as a function of physical conditions. J Metamorph Geol 20:697–708

Dale J, Holland T, Powell R (2000) Hornblende-garnet-plagioclase thermobarometry: a natural assemblage calibration of the thermodynamic of hornblende. Contrib Mineral Petrol 140:353–362

De Capitani C, Brown TH (1987) The computation of chemical equilibrium in complex systems containing non-ideal solutions. Geochim Cosmochim Acta 51:2639–2652

Devyatykh GG, Pryakhin DA, Bulanov AD, Balabanov VV (1999) Phase diagram of silicon tetrafluoride. Dokl Chem 364:75–76

Dewing EW (1997) Thermodynamics of the system NaF-AlF_3: Part VII. Non-stoichiometric solid cryolite. Metall Mater Trans 28B:1095–1097

Dolejš D, Štemprok M (2001) Magmatic and hydrothermal evolution of Li-F granites: Cínovec and Krásno intrusions, Krušné hory batholith, Czech Republic. Bull Czech Geol Surv 76:77–99

Eriksson G, Wu P, Pelton AD (1993) Critical evaluation and optimization of the thermodynamic properties and phase diagrams of the MgO-Al_2O_3, MnO-Al_2O_3, FeO-Al_2O_3, Na_2O-Al_2O_3 and K_2O-Al_2O_3 systems. CALPHAD 17:189–205

Faerøyvik M, Grand T, Julsrud S, Seltveit A (1999) Phase relations in the system NaF-CaF_2-$NaAlSiO_4$-$CaAl_2Si_2O_8$. J Am Ceram Soc 82:190–196

Förster HJ, Tischendorf G, Trumbull RB, Gottesmann B (1999) Late-collisional granites in the Variscan Erzgebirge, Germany. J Petrol 40:1613–1645

Foster PA Jr (1970) Phase equilibria in the system Na_3AlF_6-AlF_3. J Am Ceram Soc 53:598–600

Foster PA Jr (1975) Phase diagram of a portion of the system Na_3AlF_6-AlF_3-Al_2O_3. J Am Ceram Soc 58:288–291

Froning JF, Richards MK, Stricklin TW, Turnbull SG (1947) Purification and compression of fluorine. J Ind Eng Chem 39:275–278

Fuhrman ML, Lindsley DH (1988) Ternary-feldspar modeling and thermometry. Am Mineral 73:201–215

Ghiorso MS, Sack RO (1995) Chemical mass transfer in magmatic processes. IV. A revised and internally consistent thermodynamic model for the interpretation and extrapolation of liquid-solid equilibria in magmatic systems at elevated temperatures and pressures. Contrib Mineral Petrol 119:197–212

Grobelny M (1977) The hydrothermal decomposition of aluminum fluoride trihydrate. Kinetics and mechanism. J Fluor Chem 9:441–448

Haapala I (1997) Magmatic and postmagmatic processes in tin-mineralized granites: topaz-bearing leucogranite in the Eurajoki rapakivi granite stock, Finland. J Petrol 38:1645–1659

Halter WE, Williams-Jones AE (1999) Application of topaz-muscovite F-OH exchange as a geothermometer. Econ Geol 94:1249–1276

Halter WE, Williams-Jones AE, Kontak DJ (1996) The role of greisenization in cassiterite precipitation at the East Kemptville tin deposit, Nova Scotia. Econ Geol 91:368–385

Halter WE, Williams-Jones AE, Kontak DJ (1998) Modeling fluid-rock interaction during greisenization at the East Kemptville tin deposit: Implications for mineralization. Chem Geol 150: 1–17

Harms E, Schmincke H-U (2000) Volatile composition of the phonolitic Laacher See magma (12,900 yr B.P.): implications for syn-eruptive degassing of S, F, Cl and H_2O. Contrib Mineral Petrol 138:84–98

Haselton HT jr, Cygan GL, D'Angelo WM (1988) Chemistry of aqueous solutions coexisting with fluoride buffers in the system K_2O-Al_2O_3-SiO_2-H_2O-F_2O_{-1} (1 kbar, 400–700 °C). Econ Geol 83:163–173

Helgeson HC, Delany JM, Nesbitt HW, Bird DK (1978) Summary and critique of the thermodynamic properties of rock-forming minerals. Am J Sci 278A:1–229

Holland T, Powell R (1991) A compensated Redlich-Kwong (CORK) equation for volumes and fugacities of carbon dioxide and water in the range 1 bar to 50 kbar and 100–1,600 °C. Contrib Mineral Petrol 109:265–273

Holland TJB, Powell R (1998) An internally consistent thermodynamic data set for phases of petrological interest. J Metam Geol 16:309–343

Holland T, Powell R (2001) Calculation of phase relations involving haplogranitic melts using an internally consistent thermodynamic dataset. J Petrol 42:673–683

Horbe MA, Horbe AC, Costi HT, Teixeira JT (1991) Geochemical characteristics of cryolite-tin-bearing granites from Pitinga mine, northwestern Brazil—a review. J Geochem Explor 40:227–249

Johnson JW, Oelkers EH, Helgeson HC (1992) SUPCRT92: A software package for calculating the standard molal thermodynamic properties of minerals, gases, aqueous species, and reactions from 1 to 5,000 bar and 0 to 1,000 °C. Comp Geosci 18:899–947

Kiseleva IA, Ogorodova LP, Sidorov YI, Khodakovsky IL (1990) Thermodynamic properties of alkali feldspars. Geokhimiya 3:406–409

Kotelnikova ZA, Kotelnikov AR (2002) Synthetic NaF-bearing fluid inclusions. Geochem Int 40:594–600

Korytov FYa, Kudrin VS, Prokof'ev VYu, Ryabenko SV (1984) Genesis of cryolite. Dokl Akad Sci Earth Sci 279:187–189

Kovalenko VI, Kovalenko NI (1984) Problems of the origin, ore-bearing and evolution of rare-metal granitoids. Phys Earth Planet Int 35:51–62

Kovalenko VI, Tsaryeva GM, Goreglyad AV, Yarmolyuk VV, Troitsky VA, Hervig RL, Farmer GL (1995) The peralkaline granite-relaed Khaldzan-Buregtey rare metal (Zr, Nb, REE) deposit, western Mongolia. Econ Geol 90:530–547

London D (1987) Internal differentiation of rare-element pegmatites: effects of boron, phosphorus, and fluorine. Geochim Cosmochim Acta 51:403–420

London D (1997) Estimating abundances of volatile and other mobile components in evolved silicic melts through mineral-melt equilibria. J Petrol 38:1691–1706

Marshall AS, Hinton RW, MacDonald R (1998) Phenocrystic fluorite in peralkaline rhyolites, Olkaria, Kenya Rift Valley. Mineral Mag 62:477–486

Menz DH, Zacharias A, Kolditz L (1988) A comparison of the thermal behaviour of α-AlF_3 and aluminium fluoride hydrates. J Therm Anal 33:811–815

Navrotsky A, Hon R, Weill DF, Henry DJ (1980) Thermochemistry of glasses and liquids in the system $CaMgSi_2O_6$-$CaAl_2Si_2O_8$-$NaAlSi_3O_8$, SiO_2-$CaAl_2Si_2O_8$-$NaAlSi_3O_8$ and SiO_2-Al_2O_3-CaO-Na_2O. Geochim Cosmochim Acta 44:1409–1423

Pauly H (1960) Paragenetic relations in the main cryolite ore of Ivigtut, south Greenland. Neues Jahrb Mineral Abh 94:121–139

Pauly H, Bailey JC (1999) Genesis and evolution of the Ivigtut cryolite deposit, SW Greenland. Meddel Grønland, Geosci 37:1–60

Pauling L (1970) General chemistry. W H Freeman & Co, San Francisco (reprinted by Dover in 1988, 959 pp)

Peacock MA (1931) Classification of igneous rock series. J Geol 39:54–67

Pelton AD (1997) Solution models. In: Sano N et al. (eds) Advanced physical chemistry for process metallurgy. Academic Press, New York, pp 87–117

Pelton AD (1999) Thermodynamic calculations of chemical solubilities of gases in oxide melts and glasses. Glastech Ber Glass Sci Technol 72:214–226

Pistorius CWFT (1966) Effect of pressure on the melting points of the sodium halides. J Chem Phys 45:3513–3519

Pollard PJ, Pichavant M, Charoy B (1987) Contrasting evolution of fluorine- and boron-rich tin systems. Miner Deposita 22:315–321

Price JD, Hogan JP, Gilbert MC, London D, Morgan GB VI (1999) Experimental study of titanite-fluorite equilibria in the A-type Mount Scott granite: implications for assessing F contents of felsic magma. Geology 27:951–954

Robie RA, Hemingway BS (1995) Thermodynamic properties of minerals and related substances at 298.15 K and 1 bar (10^5 Pascals) pressure and at higher temperatures. USGS Bull 2131:1–461

Rutlin J (1998) Chemical reactions and mineral formation during sodium aluminium fluoride attack on aluminosilicate and anorthite based refractories. Dissertation, Norwegian University of Science and Technology, 167 pp

Ryabchikov ID, Solovova IP, Babanskii AD, Fauzi K (1996) Fluorine mobilization and bonding at magmatic and post-magmatic stages in rare-metal granites: evidence from the Homrat Akarem deposit (Egypt). Geochem Int 34:347–350

Ryabenko SV, Demina NP, Naumova IS (1988) New data on ralstonite. Nov Dann Mineral 35:204–211

Sallet R (2000) Fluorine as a tool in the petrogenesis of quartz-bearing magmatic associations: applications of an improved F-OH biotite-apatite thermometer grid. Lithos 50:241–253

Shand SJ (1927) Eruptive rocks: their genesis, composition, and classification with a chapter on meteorites. Wiley, New York, 360 pp

Shannon RD (1976) Revised effective ionic radii and systematic studies of interatomic distances in halides and chalcogenides. Acta Cryst A32:751–767

Štemprok M (1987) Greisenization (a review). Geol Rundsch 76:169–175

Štemprok M (1991) Ongonite from Ongon Khairkhan, Mongolia. Mineral Petrol 43:255–273

Stormer JC jr, Carmichael ISE (1970) Villiaumite and the occurrence of fluoride minerals in igneous rocks. Am Mineral 55:126–134

Strunz H, Nickel EH (2001) Strunz mineralogical tables. E Schweizerbart'sche Buchverhandlung, Stuttgart, 870 pp

Sverjensky DA, Hemley JJ, D'Angelo WM (1991) Thermodynamic assessment of hydrothermal alkali feldspar-mica-aluminosilicate equilibria. Geochim Cosmochim Acta 55:989–1004

Symonds RB, Reed MH (1993) Calculation of multicomponent chemical equilibria in gas-solid-liquid systems: calculation methods, thermochemical data, and applications to studies of high-temperature volcanic gases with examples from Mount St. Helens. Am J Sci 293:758–864

Thomas R, Klemm W (1997) Microthermometric study of silicate melt inclusions in Variscan Granites from SE Germany: volatile contents and entrapment conditions. J Petrol 38:1753–1765

Thomas R, Webster JD, Heinrich W (2000) Melt inclusions in pegmatite quartz: complete miscibility between silicate melts and hydrous fluids at low pressure. Contrib Mineral Petrol 139:394–401

von Wartenberg H, Bosse O (1922) Vapor pressure of some salts. III. Zeitschr Elektrochem Angew Physikal Chem 28:384–387

Webster JD, Duffield WA (1994) Extreme halogen abundances in tin-rich magma of the Taylor Creek Rhyolite, New Mexico. Econ Geol 89:840–850

Webster JD, Rebbert CR (2001) The geochemical signature of fluid-saturated magma determined from silicate melt inclusions in Ascension Island granite xenoliths. Geochim Cosmochim Acta 65:123–136

Webster JD, Thomas R, Rhede D, Förster H-J, Seltmann R (1997) Melt inclusions in quartz from an evolved peraluminous pegmatite: Geochemical evidence for strong tin enrichment in fluorine-rich and phosphorus-rich residual liquids. Geochim Cosmochim Acta 61:2589–2604

Wen S, Nekvasil H (1994) SOLVCALC: an interactive graphics program package for calculating the ternary feldspar solvus and for two-feldspar geothermometry. Comp Geosci 20:1025–1040

Willgallis A (1969) Beitrag zum System SiO_2-Na_2O-NaF. Glastech Ber 42:506–509

Williams TJ, Candela PA, Piccoli PM (1997) Hydrogen-alkali exchange between silicate melts and two-phase aqueous mixtures; an experimental investigation. Contrib Min Petrol 128:114–126

Witt WK (1988) Evolution of high-temperature hydrothermal fluids associated with greisenization and feldspathic alteration of a tin-mineralized granite, northeast Queensland. Econ Geol 83:310–334

Wu P, Eriksson G, Pelton AD (1993) Optimization of the thermodynamic properties and phase diagrams of the Na_2O-SiO_2 and K_2O-SiO_2 systems. J Am Ceram Soc 76:2059–2064

Zhu C, Sverjensky DA (1991) Partitioning of F-Cl-OH between minerals and hydrothermal fluids. Geochim Cosmochim Acta 55:1837–1858